BRAIN
A JOURNAL OF NEUROLOGY

Altered inhibitory synapses in *de novo GABRA5* and *GABRA1* mutations associated with early onset epileptic encephalopathies

Ciria C. Hernandez,[1,2,]* Wenshu XiangWei,[3,4,]* Ningning Hu,[1] Dingding Shen,[5,6] Wangzhen Shen,[1] Andre H. Lagrange,[1,7] Yujia Zhang,[8] Lifang Dai,[8] Changhong Ding,[8] Zhaohui Sun,[9] Jiasheng Hu,[10] Hongmin Zhu,[10] Yuwu Jiang[3,4,#] and Robert L. Macdonald[1,#]

*,#These authors contributed equally to this work.

We performed next generation sequencing on 1696 patients with epilepsy and intellectual disability using a gene panel with 480 epilepsy-related genes including all GABA$_A$ receptor subunit genes (GABRs), and we identified six *de novo* GABR mutations, two novel *GABRA5* mutations (c.880G>T, p.V294F and c.1238C>T, p.S413F), two novel *GABRA1* mutations (c.778C>T, p.P260S and c.887T>C, p.L296S/c.944G>T, p.W315L) and two known *GABRA1* mutations (c.335G>A, p.R112Q and c.343A>G, p.N115D) in six patients with intractable early onset epileptic encephalopathy. The α5(V294F and S413F) and α1(P260S and L296S/W315L) subunit residue substitutions were all in transmembrane domains, while the α1(R112Q and N115R) subunit residue substitutions were in the N-terminal GABA binding domain. Using multidisciplinary approaches, we compared effects of mutant GABA$_A$ receptor α5 and α1 subunits on the properties of recombinant α5β3γ2 and α1β3γ2 GABA$_A$ receptors in both neuronal and non-neuronal cells and characterized their effects on receptor clustering, biogenesis and channel function. GABA$_A$ receptors containing mutant α5 and α1 subunits all had reduced cell surface and total cell expression with altered endoplasmic reticulum processing, impaired synaptic clustering, reduced GABA$_A$ receptor function and decreased GABA binding potency. Our study identified *GABRA5* as a causative gene for early onset epileptic encephalopathy and expands the mutant *GABRA1* phenotypic spectrum, supporting growing evidence that defects in GABAergic neurotransmission contribute to early onset epileptic encephalopathy phenotypes.

1 Department of Neurology, Vanderbilt University Medical Center, Nashville, TN, USA
2 Life Sciences Institute, University of Michigan, Ann Arbor, MI, USA
3 Department of Pediatrics and Pediatric Epilepsy Center, Peking University First Hospital, Beijing, 100034, China
4 Center of Epilepsy, Beijing Institute for Brain Disorders, Beijing 100069, China
5 The Graduate Program of Neuroscience, Vanderbilt University, Nashville, TN, USA
6 Department of Neurology, Rui Jin Hospital, Shanghai Jiao Tong University, School of Medicine. Shanghai 200025, China
7 Department of Pharmacology and Molecular Physiology and Biophysics, Vanderbilt University, and the Veterans Affairs Tennessee Valley Healthcare System, Nashville, TN, USA
8 Department of Neurology, Beijing Children's Hospital, Capital Medical University, National Center for Children's Health, Beijing 100045, China
9 Epilepsy center of Yuquan Hospital, Tsinghua University, Beijing 100040, China
10 Department of Neurology, Wuhan Children's Hospital, Tongji Medical College, Huazhong University of Science and Technology, Wuhan 430016, China

Correspondence to: Ciria C. Hernandez, MD, PhD
Life Sciences Institute
University of Michigan
210 Washtenaw Ave. Room 6115
Ann Arbor, MI 48109–2216, USA
E-mail: ciria@umich.edu

Correspondence may also be addressed to: Robert L Macdonald, MD, PhD
Department of Neurology
Vanderbilt University Medical Center
465 21st Ave. South. MRB III, Suite 6140
Nashville, TN - 37240–7915, USA
E-mail: robert.macdonald@vumc.org

Yuwu Jiang, MD, PhD
Department of Pediatrics and Pediatric Epilepsy Center
Peking University First Hospital
No.1 Xi'an Men Street, West District
Beijing 100034, China
E-mail: jiangyuwu@bjmu.edu.cn

Introduction

Epileptic encephalopathies are a heterogeneous group of epilepsy syndromes associated with severe recurrent seizures and neurodevelopmental impairment (Helbig and Tayoun, 2016). Early onset epileptic encephalopathies (EOEE) are invariably associated with seizure onset occurring during the first few years of life, cognitive regression and intellectual disability (Nieh and Sherr, 2014). Twenty-five to 40% of them have no known acquired cause, and their EOEE syndrome is thought to have a genetic aetiology (McTague *et al.*, 2016; Axeen and Olson, 2018). Next-generation sequencing data have indicated that sporadic *de novo* mutations are a major cause of these disorders (Hamdan *et al.*, 2017). Further, more than 30 genes have been strongly established as causative for genetic epileptic encephalopathies (Helbig *et al.*, 2016, 2017). *De novo* pathogenic mutations in the GABA$_A$ receptor α1 subunit gene (*GABRA1*) have been associated with a broad phenotypic range of severe epileptic encephalopathies including Ohtahara syndrome, infantile spasms, myoclonic astatic epilepsy (Doose syndrome) and Dravet syndrome (Johannesen *et al.*, 2016; Kodera *et al.*, 2016). In addition, the epilepsy phenotypic spectrum of *de novo* mutations in GABA$_A$ receptor β3 and γ2 subunit genes (*GABRB3* and *GABRG2*, respectively) include Lennox-Gastaut syndrome, infantile spasms and Dravet syndrome (Allen *et al.*, 2013; Hamdan *et al.*, 2014; Hernandez *et al.*, 2017*a*, *b*; Le *et al.*, 2017; Moller *et al.*, 2017; Shen *et al.*, 2017). Conversely, no association of *GABRA5* and EOEE has been established.

GABA$_A$ receptor α subunits show high levels of structural conservation with β and γ subunits (Hibbs and Gouaux, 2011; Miller and Aricescu, 2014; Du *et al.*, 2015; Laverty *et al.*, 2019). All six *de novo* mutations identified in our cohort produced residue changes clustered within or in close proximity to the GABA-binding pocket (*GABRA1*: c.G335A, p.R112Q and c.A343G, p.N115D) or transmembrane domains forming the ion channel pore of the receptor (*GABRA5*: c.G880T, p.V294F and c.C1238T, p.S413F; *GABRA1*: c.T778C, p.P260S and c.T887C, p.L296S; c.G944T, p.W315L) (Table 1). Indeed, we and others have reported mutations in other GABRs that change residues in the N-terminal domain as well as the pore region of GABA$_A$ receptors (Huang *et al.*, 2014; Hernandez *et al.*, 2016, 2017*a*, *b*; Janve *et al.*, 2016; Ishii *et al.*, 2017; Shen *et al.*, 2017). The *de novo* GABRA1 p.R112Q and p.N115D residue substitutions have been detected recurrently in unrelated patients within the previous cohort studies (Carvill *et al.*, 2014; Johannesen *et al.*, 2016; Kodera *et al.*, 2016). Clustering of *de novo* mutations in *GABRA* that code for canonical domains of GABA$_A$ receptor α subunits, which are closely related to the gating of the channel, might result in impaired inhibitory synaptic transmission. We hypothesized that common synaptic defects that are likely to modulate GABAergic network excitability are altered in patients carrying EOEE-associated *GABRA5* and *GABRA1* mutations.

Materials and methods

Patient phenotypes

A cohort of 1969 patients with epilepsy and intellectual disability were screened by a gene panel targeting 480

Table 1 Pathogenicity prediction of *GABRA5* and *GABRA1* missense mutations in six individuals with EOEE

Gene	SNPs	Protein substitution	Sequence conservation	Structural domain	PolyPhen-2	SIFT	MutationTaster	ExAC	Recurrence
GABRA5	c.880G>T	p.V294F	Conservative	Pore (M2)	Probably damaging	Deleterious	Disease causing	NF	Novel[a]
GABRA5	c.1238C>T	p.S413F	Non-conservative	Intracellular (N-tail M4)	Benign	Tolerated	Polymorphism	NF	Novel
GABRA1	c.335G>A	p.R112Q	Non-conservative	Binding (β3 strand)	Benign	Tolerated	Disease causing	NF	Six cases[b]
GABRA1	c.343A>G	p.N115D	Non-conservative	Binding (α3 helix)	Probably damaging	Tolerated	Disease causing	NF	Two cases[c]
GABRA1	c.778C>T	p.P260S	Identical	Pore (M1)	Probably damaging	Deleterious	Disease causing	NF	Novel[d]
GABRA1	c.887T>C	p.L296S	Non-conservative	Pore (M2)	Probably damaging	Deleterious	Disease causing	NF	Novel
GABRA1	c.944G>T	p.W315L	Non-conservative	Pore (M3)	Probably damaging	Tolerated	Disease causing	NF	Novel

[a]One unrelated case with severe epilepsy and developmental delay were described by Butler *et al.* (2018) with the *de novo* p.Val294Leu variant.
[b]Six unrelated cases reported by Carvill *et al.* (2014) (two cases), Kodera *et al.* (2016) (one case), Johannesen *et al.* (2016) (two cases) and the present study (one case).
[c]Two unrelated cases reported by Johannesen *et al.* (2016) (one case) and the present study (one case).
[d]Two unrelated cases with Ohtahara and West syndromes were described by Kodera *et al.* (2016) with the *de novo* p.Pro260Leu substitutions.
NF = not found.

Table 2 Clinical features in two individuals with EOEE and *GABRA5* missense mutations

	Patient 1	Patient 2
Inheritance	*De novo*	*De novo*
Amino acid change	V294F	S413F
Sex	Male	Male
Diagnosis	EOEE	EOEE
Current age	3 years, 10 months	7 years
Age at onset	4 months	3 months
Seizure types	Focal seizures with generalization, febrile seizures, and status epilepticus	Focal and tonic seizures. Epileptic spasms
EEG	Generalized slow waves in background activity. Multifocal sharp waves during attack period	Spams in clusters with focal seizures and hypsarrhythmia
Motor development	Severe delay	Severe delay
Cognitive outcome	Severe intellectual disability	Severe intellectual disability
MRI findings	Frontotemporal atrophy and thin corpus callosum	Cortical atrophy and thin corpus callosum

epilepsy-related genes that included all GABA_A receptor subunit genes (GABRs) (Hernandez *et al.*, 2017*b*). The patients were recruited from the Department of Pediatrics at the Peking University First Hospital from 2006 to 2015. Clinical work-up of all patients showed no definite perinatal brain injury, no hypoxia, and ischaemia, infection of the CNS or cranial trauma. No evidence of typical inherited metabolic disorders or specific neurodegenerative disorders based on clinical features, neuroimaging or blood/urinary metabolic diseases screening were found. Additionally, normal routine karyotyping and the detection of chromosome sub-telomeric rearrangements with multiplex ligation-dependent probe amplification (MLPA) showed no abnormalities, strongly suggesting a genetic aetiology. Six *de novo GABRA1* and *GABRA5* mutations were identified in six patients who were clinically diagnosed as having epilepsy and severe intellectual disability of unknown origin and diagnosed as EEOE (Tables 2 and 3). The parents in the six trios had no epilepsy or any related history. All genomic DNA used in the experiments was extracted from peripheral leucocytes. The study was approved by the Ethics committee of Peking University First Hospital, and written informed consents were obtained from all patients or their legal guardians.

Next generation sequencing and variant validation analysis

The gene panel targeted 480 epilepsy-related genes found in several databases (OMIM, www.omim.org; HGMD, www.hgmd.cf.ac.uk; and EpilepsyGene, http://61.152.91.49/EpilepsyGene/) that were synthesized using the Agilent SureSelect Target Enrichment technique (Zhongguancun Huakang Gene Institute, China) (Hernandez *et al.*, 2017*b*). We used the American College of Medical Genetics and Genomics (ACMG) guidelines to evaluate the pathogenicity of mutations before they were selected for functional study. Missense mutations were cross-validated according to known polymorphism databases including the 1000 Genomes project (Abecasis *et al.*, 2012), ESP (Exome Variant Server), ExAC (Exome Aggregation Consortium) (Lek *et al.*, 2016) and Ensembl (Aken *et al.*, 2016) (Human_GRCh37/hg19). In addition to determining population frequency, the four *GABRA1*

Table 3 Clinical features in four individuals with EOEE and *GABRA1* missense mutations

	Patient 1	Patient 2	Patient 3	Patient 4
Inheritance	*De novo*	*De novo*	*De novo*	*De novo*
Amino acid change	R112Q	N115D	P260S	L296S/W315L
Sex	Male	Male	Female	Female
Diagnosis	EOEE	EOEE	West syndrome	West syndrome
Current age	19 years	4 years, 5 months	3 years, 1 month	5 years, 9 months
Age at onset	8 months	12 months	4 months	8 months
Seizure types	Partial seizures, generalized tonic clonic seizures	Partial seizures, generalized tonic clonic seizures, febrile seizures.	Epileptic spasms	Epileptic spasms
EEG	Persistent diffuse slow background activity	Generalized discharges during seizures	Spams in clusters and hypsarrhythmia	Hypsarrhythmia or atypical hypsarrhythmia
Motor development	Nearly normal	Mild delay	Severe delay	Severe delay
Cognitive outcome	Severe intellectual disability	Severe intellectual disability	Severe intellectual disability	Severe intellectual disability
MRI findings	Cortical atrophy[a]	Thin bilateral para-hippocampal gyrus	Thin corpus callosum	Frontotemporal atrophy

[a]CT scan.

and two *GABRA5* variants identified in the patient were filtered for call quality and frequency in the Genome Aggregation Database (gnomAD). They were all absent from gnomAD, supporting their pathogenicity. More than 98% of targets had at least $30\times$ (average $136\times$) coverage. Validation of suspicious mutations as well as segregation analysis in both parents of the six patients were performed by *post hoc* standard Sanger sequencing. Subsequent parental testing revealed the mutations to be *de novo*. Deleterious impact of missense mutations on protein structure and DNA sequence alterations were scored with PolyPhen-2 (Adzhubei *et al.*, 2010), SIFT (Ng and Henikoff, 2001) and MutationTaster (Schwarz *et al.*, 2010) (Table 1).

DNA constructs

The coding sequences of human $\alpha 5$ (NM_000810.3), $\alpha 1$ (NM_000806.5), $\beta 3$ (NM_021912.4) and $\gamma 2L$ (NM_198904.2) GABA$_A$ receptor subunits and EGFP (LC008490.1) were cloned into pcDNA3.1(+) expression vectors (Invitrogen). Mutant $\alpha 5$ and $\alpha 1$ subunit cDNA constructs were generated using the QuikChange Site-Directed Mutagenesis Kit (Agilent) and confirmed by DNA sequencing. The haemagglutinin (HA) epitope was inserted between the fourth and fifth residue of the mature $\alpha 5$ subunit, a functionally silent position (Connolly *et al.*, 1996).

Primary hippocampal neuronal culture

Rat hippocampal neurons were obtained from embryonic Day 17.5 embryos. Briefly, dissociated cells were plated at a density of 6.5×10^4 cells/cm^2 onto 12-mm round coverslips in 24-well plates coated with poly-L-ornithine (0.5 mg/ml; Sigma). Hippocampal neurons were incubated at 37°C in a 5% CO$_2$ incubator and maintained in serum-free Neurobasal^{TM} medium (Gibco) supplemented with B27 supplement (Gibco), glutamine (Gibco) and penicillin/streptomycin (Gibco, 20 U/ml). For electrophysiology studies, hippocampal neurons were transfected at days *in vitro* (DIV) 7 with 2 μg of wild-

type or mutant subunits and 0.5 μg of EGFP using X-tremeGENE^{TM} 9 DNA transfection reagent, and recordings were obtained at DIV 14–19. For confocal studies, hippocampal neurons were transfected at DIV 10 using Lipofectamine$^{®}$ 2000 transfection reagent (Invitrogen) and imaging was obtained at DIV 12.

Non-neuronal cell culture

HEK293T cells (ATCC, CRL-11268) were cultured at 37°C in a humidified 5% CO$_2$ incubator and maintained in Dulbecco's modified Eagle medium (Invitrogen) supplemented with 10% foetal bovine serum (Life Technologies) and 100 IU/ml penicillin/streptomycin (Life Technologies). For western blot and surface biotinylation experiments, cells were transfected using polyethylenimine (PEI) reagent (40 kD, Polysciences) at a DNA:transfection reagent ratio of 1:2.5, and harvested 36 h after transfection. To express wild-type and mutant $\alpha 5\beta 3\gamma 2$ and $\alpha 1\beta 3\gamma 2$ receptors, 3 μg of subunit DNAs were transfected at a ratio of 1:1:1 into 6 cm dishes for most experiments except for whole-cell recording. For the mock-transfected condition, empty pcDNA3.1 vector was added to make a final DNA transfection amount of 3 μg. Whole cell recordings were obtained from HEK293T cells plated onto 12 mm coverslips at a density of 4×10^4 in 35 mm culture dishes (Corning) and transfected after 24 h with 0.3 μg cDNA of each $\alpha 5$, $\alpha 1$, $\beta 3$ and $\gamma 2$ subunit, and 0.05 μg of EGFP using X-tremeGENE^{TM} 9 DNA transfection reagent (Roche Diagnostics). Recordings were obtained 48 h after transfection.

Immunocytochemistry and confocal microscopy

Coverslip-grown hippocampal neurons or HEK293T cells were fixed with Prefer (Anatech) and permeabilized with 0.2% Triton^{TM} X-100 for 15 min to stain total proteins. The fixed/permeabilized cells were blocked for 2 h with 5% bovine serum albumin in phosphate-buffered saline and then stained

with primary antibodies overnight, followed by incubation in Alexa 488-conjugated donkey anti-rabbit IgG antibodies and Cy3-conjugated donkey anti-mouse IgG antibodies. Primary antibodies used were as follows: rabbit monoclonal HA antibody (Cell Signaling), mouse monoclonal HA antibody (BioLegend), rabbit polyclonal MAP2 antibody (Cell Signaling), mouse monoclonal anti-gephyrin antibody (Synaptic Systems), mouse monoclonal anti-calnexin antibody (Abcam). Coverslips were mounted with ProLong® Gold antifade reagent (Thermo Fisher Scientific).

Confocal images were obtained using a Zeiss LSM 710 Meta inverted confocal microscope. Stained hippocampal neurons or HEK293T cells were excited with the 488 nm laser for the Alexa 488 fluorophore signal and the 543 nm laser for the Cy3 fluorophore signal. Co-localization analysis of hippocampal neurons was performed using the Coloc2 plugin in the open source image processing program Fiji (Schindelin *et al.*, 2012). Both Pearson's correlation coefficient (R) and Manders' co-localization coefficient (MCC) were calculated (Shen *et al.*, 2017).

Western blot and surface biotinylation of non-neuronal cells

Transfected HEK293T cells were collected in modified RIPA buffer [50 mM Tris (pH = 7.4), 150 mM NaCl, 1% NP-40, 0.2% sodium deoxycholate, 1 mM EDTA] and 1% protease inhibitor cocktail (Sigma). Collected samples were subjected to gel electrophoresis using 4–12% BisTris NuPAGE precast gels (Invitrogen) and transferred to PVDF-FL membranes (Millipore). Primary antibodies against human $\alpha5$ (Millipore), $\alpha1$ (NeuroMab), $\beta3$ (Novus Biologicals), and $\gamma2$ subunits (Millipore) were used to detect the subunits at a 1:500 dilution. Anti-Na^+/K^+ ATPase antibody (Developmental Studies Hybridoma Bank) at a 1:1000 dilution was used as a loading control. IRDye® (LI-COR Biosciences) conjugated secondary antibody was used at a 1:10 000 dilution in all cases. Membranes were scanned using the Odyssey Infrared Imaging System (LI-COR Biosciences). The integrated density value of bands was determined using the Odyssey Image Studio software (LI-COR Biosciences) (Hernandez *et al.*, 2017a, b).

GABA-evoked currents of non-neuronal cells

Whole-cell recordings of wild-type and mutant $GABA_A$ receptor currents were obtained at room temperature from lifted HEK293T cells (Hernandez *et al.*, 2017a, b). The external solution was composed of (in mM): 142 NaCl, 8 KCl, 10 D(+)-glucose, 10 HEPES, 6 $MgCl_2.6H_2O$, and 1 $CaCl_2$ (pH 7.4, ~326 mOsm). The internal solution consisted of (in mM): 153 KCl, 10 HEPES, 5 EGTA 2 Mg-ATP, and 1 $MgCl_2.6H_2O$ (pH 7.3, ~300 mOsm). GABA (1 mM) was applied for 4 s for measurements of current amplitude. The currents were recorded using an Axopatch 200B amplifier (Axon Instruments), low-pass filtered at 2 kHz using the internal 4-Pole Bessel filter of the amplifier, digitized at 10 kHz with Digidata 1550 (Axon Instruments) and stored for offline analysis as described previously.

$GABA_A$ receptor-mediated miniature inhibitory postsynaptic currents

Miniature inhibitory postsynaptic currents were recorded from DIV 14–21 cultured hippocampal neurons (Hernandez *et al.*, 2017a). Whole-cell patch-clamp recordings were obtained at room temperature (22–23°C) at a holding potential of −60 mV. Hippocampal neurons were perfused with an extracellular solution containing 145 mM NaCl, 3 mM KCl, 1.5 mM $CaCl_2$,1 mM $MgCl_2.6H_2O$, 10 mM glucose, and 10 mM HEPES (pH 7.4, ~320 mOsm). The internal solution consisted of 135 mM CsCl, 2 mM $MgCl_2.6H_2O$, 10 mM EGTA, 5 Mg-ATP, and 10 mM HEPES (pH 7.2, ~300 mOsm). $GABA_A$ receptor-mediated mIPSCs were recorded by blocking both action potentials and excitatory neurotransmission. Thus, tetrodotoxin (TTX, 0.5 µM), d(−)-2-amino-5-phosphonopentanoate (AP5, 40 µM), and 6-cyano-7-nitroquinoxaline-2,3-dione (CNQX, 10 µM) were added the extracellular solution.

Statistical analysis

Numerical data were reported as mean ± standard error of the mean (SEM). Statistical analysis was performed using GraphPad Prism (GraphPad Software 6.07). Statistically significant differences were taken as $P < 0.05$ using one-way ANOVA followed by Dunnett's multiple comparison test.

Data availability

The data supporting the findings of this study are available within the article and its Supplementary material.

Results

Patient phenotypes with *de novo* *GABRA5* missense mutations found in cases with EOEE

The clinical features of the two patients with *GABRA5* mutations are summarized in Table 2, and their representative EEG and brain MRI images presented in Fig. 1A and B. Both patients were diagnosed with EOEE. The seizures began within the first 4 months of life. Seizure semiology at onset was described as partial seizures with secondary generalization, febrile seizures and status epilepticus in Patient 1, and epileptic spasms and tonic seizures in Patient 2. A variety of EEG abnormalities were found in Patient 1 including generalized slow-wave epileptiform discharges and multifocal sharp waves (Fig. 1A). Patient 2 showed some symptoms of Ohtahara syndrome at an early age, which were evolving towards symptoms of infantile spasms and West syndrome at a later age. Figure 1B showed an abnormal interictal pattern on EEG (i.e. hypsarrhythmia at 5 months) found in Patient 2 at 5 months old. Brain MRIs showed cortical atrophy and thinning of the corpus callosum (Fig. 1A and B). Seizures remained

intractable as of last follow up despite combination therapy with antiepileptic drugs for both patients. Developmentally, these patients had severe intellectual disability, were non-verbal and had severe motor disabilities.

Patient phenotypes with *de novo GABRA1* missense mutations found in cases with EOEE

The clinical features of the four patients with *GABRA1* mutations were summarized in Table 3. Representative EEG and brain MRI images of Patients 3 and 4 are shown in Fig. 1C and D. The age of onset of epilepsy was within the first year of life in all four patients (range 4 to 12 months of age). Seizure semiologies at onset were described as partial seizures with secondary generalized tonic-clonic seizures in Patients 1 and 2, epileptic spasms in Patient 3 (Fig. 1C), and myoclonic seizures in Patient 4 (Fig. 1D). These patients were examined frequently to determine if they fit criteria for a specific EEG syndrome diagnosis (i.e. hypsarrhythmia). Patients 1 and 2 were diagnosed with EOEE, and Patients 3 and 4 eventually had features of West syndrome when multiple individual spasms were observed. Epilepsy outcome was variable, with Patient 1 eventually becoming seizure free for nearly 1 year after a conventional antiepileptic drug combination of pentobarbital, valproic acid, clonazepam and phenytoin. Patient 3 responded poorly to antiepileptic drugs, but epileptic spasms were reduced by a combination of adrenocorticotropic hormone and $MgSO_4$. In contrast, the seizures in Patients 2 and 4 remained intractable despite combination therapy with antiepileptic drugs. Developmentally, all four individuals had severe intellectual disability, were nonverbal, and had different degrees of motor disabilities, ranging from nearly normal (Patient 1) to mild (Patient 2) or to severe motor delay (Patients 3 and 4). A variety of interictal epileptiform discharges were observed on EEGs in this cohort including persistent diffuse slow background activity (Patient 1), generalized discharges (Patient 2), hypsarrhythmia (Patients 3 and 4), and bilateral multi-spikes (all patients). Brain MRIs (Patients 2–4) and CT scan (Patient 1) were abnormal in all patients (Fig. 1C and D shows only Patients 3 and 4).

Altered synaptic distribution and gephyrin clustering of two novel EOEE mutant α5 subunits in primary hippocampal neurons

To determine whether $GABA_A$ receptors containing EOEE-associated mutant α5(V294F) or α5(S413F) subunits had defective synaptic localization in dendrites, we expressed HA-fusion-proteins encoding wild-type α5 subunits or mutant α5(V294F) or α5(S413F) subunits in hippocampal neurons (DIV 12). We used double immunostaining for MAP2 and HA to demonstrate that α5 subunit-containing $GABA_A$ receptors formed clusters at GABAergic synapses in dendrites of cultured hippocampal neurons (Fig. 2A). On dendrites we observed a marked decrease of puncta containing HA in neurons expressing mutant α5(V294F)[HA] subunits compared with those expressing wild-type α5 subunits (Fig. 2A). In contrast, in neurons expressing mutant α5(S413F)[HA] subunits, the dendrites displayed numerous synaptic contacts containing HA, similar to those observed in neurons expressing wild-type α5 subunits.

We then asked whether the reduction of dendritic expression of mutant α5(V294F) subunit-containing receptors altered the efficacy of GABAergic inhibition of hippocampal neurons (Fig. 2B). We measured $GABA_A$ receptor-mediated mIPSCs in neurons transfected with wild-type α5 subunits and those transfected with mutant α5(V294F) or α5(S413F) subunits recorded in the presence of TTX, AP5, and CNQX to block voltage-gated sodium channels and glutamate receptors, respectively.

As expected, mean mIPSC amplitude in hippocampal neurons transfected with mutant α5(V294F)[HA] subunits was significantly decreased (11.5 ± 1.6 pA, $P = 0.0001$, $n = 5$) relative to that of neurons transfected with wild-type α5 subunits (25.2 ± 1.7 pA, $n = 5$). Further, mean mIPSC amplitude in hippocampal neurons transfected with mutant α5(S413F) subunits was significantly reduced (18.5 ± 0.4 pA, $P = 0.0086$, $n = 5$) relative to hippocampal neurons transfected with wild-type α5 subunits (25.2 ± 1.7 pA) (Fig. 2B, bottom left).

The decay time of mIPSCs in neurons transfected with mutant α5(V294F) subunits was decreased (28.30 ± 4.02 ms, $P = 0.0001$, $n = 5$), but the decay time of mIPSCs in neurons transfected with mutant α5(S413F) subunits (72.11 ± 5.17 ms, $P = 0.1608$, $n = 5$) was similar to the decay time of mIPSCs in neurons transfected with wild-type α5 subunits (82.96 ± 3.20 ms, $n = 5$) (Fig. 2B, bottom middle).

The rise time of mIPSCs in neurons transfected with mutant α5(S413F) subunits was increased (5.54 ± 0.81 ms, $P = 0.0347$, $n = 5$), but the rise time of mIPSCs in neurons transfected with mutant α5(V294F) subunits (3.32 ± 0.61 ms, $P = 0.9608$, $n = 5$) was similar to that of mIPSCs in neurons transfected with wild-type α5 subunits (3.11 ± 0.41 ms, $n = 5$) (Fig. 2B, bottom right). These results demonstrated that the decreased dendritic puncta caused by mutant α5(V294F) subunits was associated with reduced GABAergic inhibition in hippocampal neurons. In contrast, the unaltered dendritic localization in neurons transfected with mutant α5(S413F)[HA] subunits did not explain the reduced GABAergic inhibition, and thus, other mechanisms must be responsible.

It is well known that α5 subunit-containing $GABA_A$ receptors are clustered at synapses by interacting with gephyrin (Christie and de Blas, 2002; Jacob *et al.*, 2005; Serwanski *et al.*, 2006). We analysed the synaptic localization of wild-type α5 subunits and mutant α5(V294F)[HA]
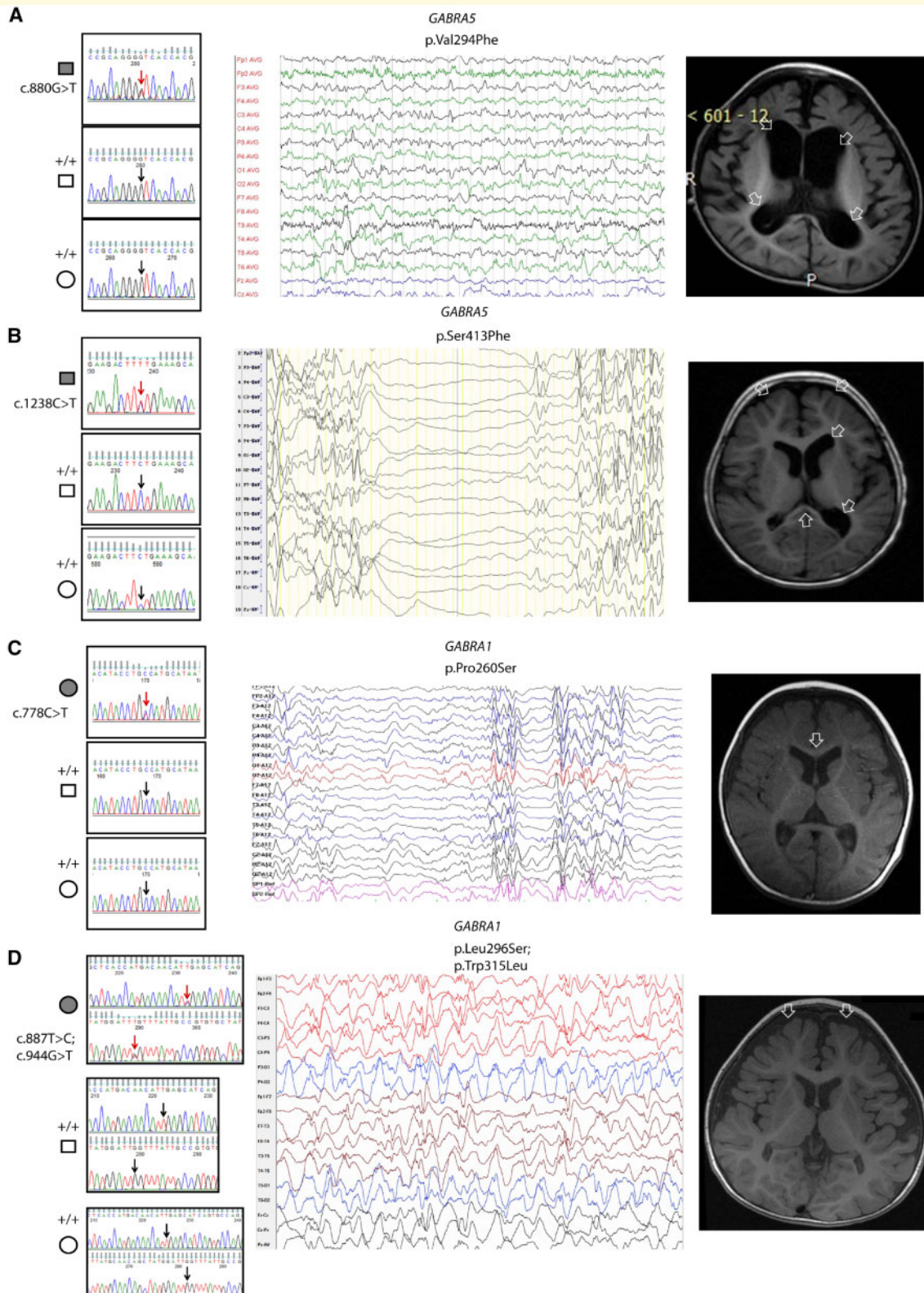
Figure 1 Novel *de novo* GABRA5 and GABRA1 mutations were identified in individuals with EOEE. Segregation analysis (*left*), representative EEGs (*middle*) and brain MRIs (*right*) are presented for patients with two novel *GABRA5* mutations (**A** and **B**) and two novel *GABRA1* mutations (**C** and **D**) that were identified in four trios (Patients 1 and 2, Table 2; Patients 3 and 4, Table 3). On the *left* of the panels, the filled symbols indicate probands, and the arrows on Sanger chromatograms indicate the missense nucleotide. Four representative EEGs are presented. The *top* EEG demonstrates generalized slow waves in background activity (**A**) and typical hypsarrhythmia (**B**). The *lower* two EEG traces show more spasms in clusters and hypsarrhythmia (**C**) and atypical hypsarrhythmia (**D**). All the patients had common abnormalities in their brain MRIs (*right*). The four patients had cortical atrophy, and thin corpus callosum as shown (open arrows). All images are presented at the level of head of caudate. On the *left* for each trio, square symbols indicate males, circles indicate females, filled symbols indicate the affected index case and the open symbols indicate the unaffected parents.
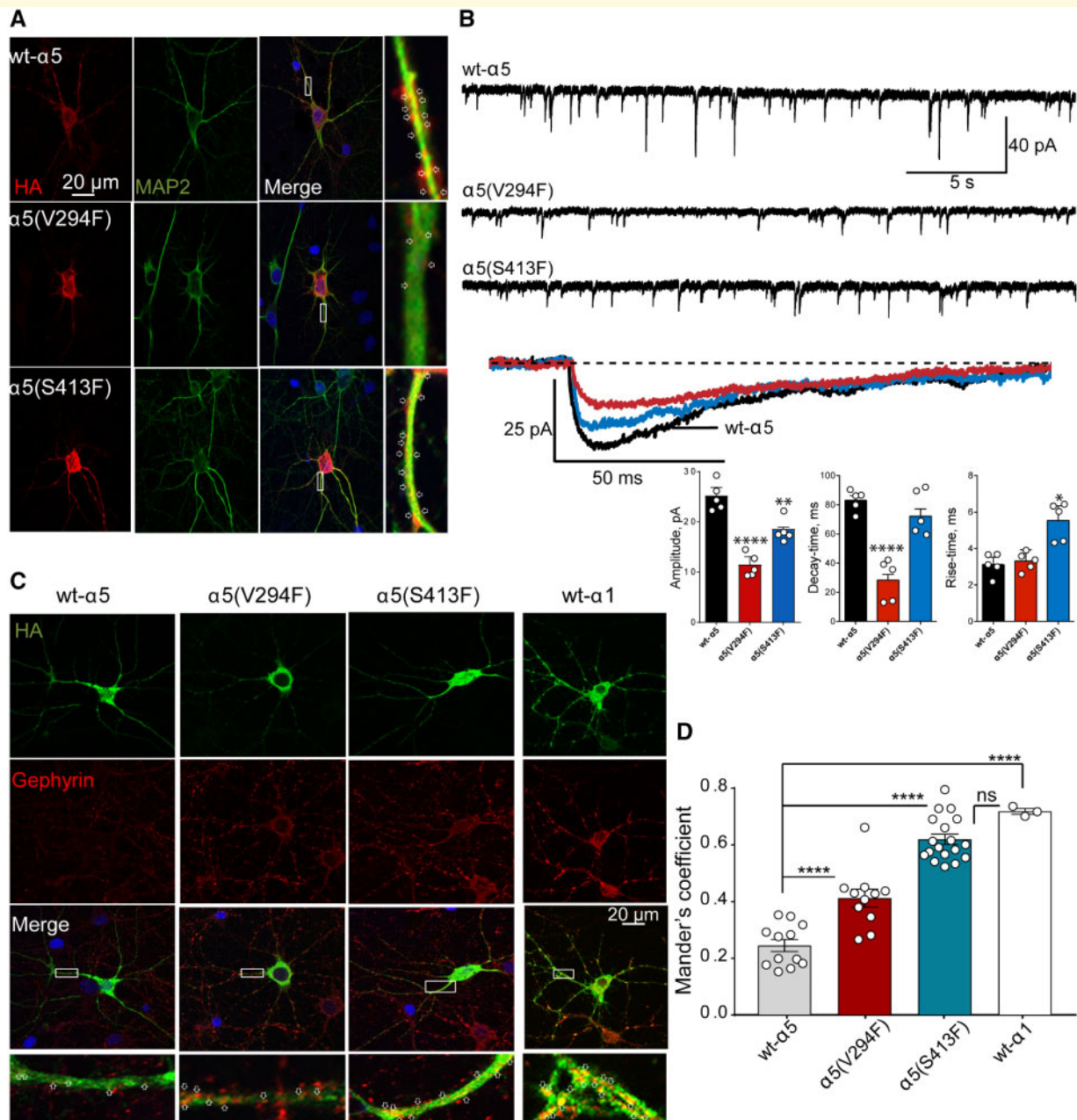
Figure 2 Altered synaptic distribution and gephyrin clustering of mutant α5 subunit-containing GABA$_A$ receptors in hippocampal neurons in cell culture. (A) Hippocampal neurons in cell culture (DIV 10) were transfected with wild-type (wt) α5^{HA}, subunits or mutant α5(V294F)^{HA} or α5 (S413F)^{HA} subunits and were fixed 48 h later. Neurons were stained with anti-HA antibodies (red) and MAP2 (green). Staining patterns were characterized using confocal microscopy. The *right* of the panel contains enlarged images of the neurites in white boxes. **(B)** Representative mISPC traces recorded at −60 mV in cultured hippocampal neurons over-expressing mutant α5(V294F)^{HA} or α5(S413F)^{HA} subunits or wild-type α5^{HA} subunits are presented. *Bottom* bar graphs represent summarized mISPC data. Values are expressed as mean ± SEM (see text). One-way ANOVA with Dunnett's post-test was used to determine significance compared to the wild-type condition. **(C)** Gephyrin clustering patterns were revealed by confocal microscopy. Neurons were stained with anti-HA (green) and anti-gephyrin (red) antibodies. The *bottom* of the panel contains enlarged images of the neurites in white boxes. **(D)** Statistical analyses of gephyrin clustering were performed using MCC. Values are expressed as mean ± SEM (see text). One-way ANOVA with Dunnett's post-test was used to determine significance compared to the wild-type condition.

and α5(S413F)^{HA} subunits in hippocampal neurons by comparing their co-localization with gephyrin (Fig. 2C and D). First, we observed an inverse relationship in the number of clusters co-localized with gephyrin and the type of α subunit-containing GABA$_A$ receptors. Endogenous wild-type α1 and exogenous wild-type α5

subunit-containing receptors were both co-localized with gephyrin, but the clusters were larger with $\alpha 1$ than with $\alpha 5$ subunit-containing receptors ($\alpha 1$-MCC = 0.72 ± 0.01, $n = 3$; $\alpha 5$-MCC = 0.25 ± 0.02, $n = 12$, $P = 0.0001$). When comparing the gephyrin clusters with mutant subunit expressing receptors, the mutant $\alpha 5$(V294F)^{HA} subunits presented more clusters than wild-type $\alpha 5$ subunits (MCC = 0.41 ± 0.03, $n = 11$, $P = 0.0001$), and the mutant $\alpha 5$(S413F) subunits had significantly more gephyrin clusters than the wild-type $\alpha 5$ subunits (MCC = 0.41 ± 0.03, $n = 11$, $P = 0.0001$) or mutant $\alpha 5$(S413F) subunits (MCC = 0.62 ± 0.02, $n = 18$, $P = 0.0001$). The high level of gephyrin clustering found in $\alpha 5$(S413F)^{HA} subunit expressing neurons was not different from that of endogenous $\alpha 1$ subunit-containing receptors ($P = 0.155$). These data suggest aberrant redistribution of $\alpha 5$ subunit-containing GABA$_A$ receptors at the synapses of both mutant $\alpha 5$(V294F)^{HA} and $\alpha 5$(S413F)^{HA} subunit-expressing neurons.

De novo EOEE mutant $\alpha 5$ subunits trafficked to cell membranes as functional receptors

We observed a differential distribution of mutant $\alpha 5$(V294F)^{HA} and $\alpha 5$(S413F)^{HA} GABA$_A$ receptor subunits in somatodendritic compartments of hippocampal neurons (Fig. 2A). While mutant $\alpha 5$(S413F)^{HA} subunits were localized primarily on the dendrites, mutant $\alpha 5$(V294F)^{HA} subunits accumulated in the soma. These results suggested impaired biogenesis of mutant $\alpha 5$(V294F)^{HA} subunits. Further, we sought to determine whether the differences in the somatodendritic distribution of mutant $\alpha 5$(V294F)^{HA} subunit-containing receptors were due to surface trafficking defects that would result in some subunit retention in the endoplasmic reticulum (ER). To assess this, we performed confocal microscopy staining of calnexin, an ER marker that exhibits a typical perinuclear and reticular distribution suggestive of an ER distribution (Fig. 3A), to co-localized mutant $\alpha 5$^{HA} subunits that did not form trafficking-competent receptors and were trapped in the ER. To assess ER retention, permeabilized HEK293T cells were immunolabelled with anti-HA and anti-calnexin antibodies. We found that mutant $\alpha 5$(V294F)^{HA} subunits predominantly localized to the ER as evidenced by their co-localization with calnexin (MCC = 0.68 ± 0.02, $n = 3$, $P = 0.0003$), in contrast to mutant $\alpha 5$(S413F)^{HA} subunits that spread outside the ER (MCC = 0.46 ± 0.03, $n = 3$, $P = 0.4115$) and showed a distribution similar to wild-type $\alpha 5$^{HA} subunits (MCC = 0.42 ± 0.01, $n = 3$), suggesting trafficking to the cell surface. Although these results indicated that there was a defect in the trafficking of GABA$_A$ receptors containing mutant $\alpha 5$(V294F)^{HA} subunits to the surface membrane, it did not totally exclude the possibility that a fraction of receptors were trafficked to the surface

membrane and remained functional, as shown in hippocampal neurons (Fig. 2B).

To shed light on the functional properties of the receptors expressed on the surface membrane, we measured macroscopic GABA-evoked currents in transfected HEK293T cells (Fig. 3B). Similar to the results shown above, transfection of cells with mutant $\alpha 5$(V294F)^{HA} and $\alpha 5$(S413F)^{HA} subunit-containing GABA$_A$ receptors decreased GABA-evoked currents to different extents. While $\alpha 5$(V294F)^{HA} subunits decreased currents by ∼39% (5241 ± 289 pA, $n = 15$, $P = 0.0001$), $\alpha 5$(S413F) subunits decreased currents by ∼24% (6498 ± 278 pA, $n = 22$, $P = 0.0009$) relative to wild-type currents (8532 ± 88 pA, $n = 6$) (Fig. 3B). Concomitantly, the sensitivity to Zn^{2+} inhibition was increased in GABA$_A$ receptors containing mutant $\alpha 5$(V294F)^{HA} subunits (25 ± 4%, $n = 10$, $P = 0.0005$). In contrast, GABA$_A$ receptors containing mutant $\alpha 5$(S413F)^{HA} subunits had a smaller fractional Zn^{2+} inhibition (14 ± 1%, $n = 16$, $P = 0.3238$), similar to that of GABA$_A$ receptors containing wild-type $\alpha 5$ subunits (9 ± 2%, $n = 8$). Unexpectedly, neither mutant $\alpha 5$(V294F)^{HA} nor mutant $\alpha 5$(S413F)^{HA} subunit altered GABA potency, and receptors containing either mutant subunit had GABA concentration-response curves with EC$_{50}$'s similar to those of GABA$_A$ receptors containing wild-type (WT) $\alpha 5$ subunits [EC$_{50}$$^{(V294F)}$ = 4.33 µM, $P = 0.6870$, $n = 6$; EC$_{50}$$^{(S413F)}$ = 5.84 µM, $P = 0.8128$, $n = 6$; EC$_{50}$$^{(WT)}$ = 5.77 µM, $n = 15$].

Taken together these results demonstrated that the *GABRA5* EOEE-associated mutations decreased GABA-evoked current amplitudes in both neuronal and non-neuronal cells due to impaired biogenesis of receptors leading to decreased or altered expression of surface receptors. To determine to what extent the mutant $\alpha 5$(V294F) and $\alpha 5$(S413F) subunits assembled with $\beta 3$ and $\gamma 2$ subunits and trafficked to cell surface membranes, we co-expressed wild-type $\alpha 5$^{HA} subunits or mutant $\alpha 5$(V294F)^{HA} or $\alpha 5$(S413F)^{HA} subunits with $\beta 3$ and $\gamma 2$ subunits in HEK293T cells and evaluated surface levels of wild-type and mutant $\alpha 5$ subunits by surface biotinylation (Fig. 3C). Compared to co-expressed wild-type $\alpha 5$ subunits, we found that surface levels of co-expressed mutant $\alpha 5$(V294F)^{HA} subunits were reduced (0.59 ± 0.04, $P = 0.0012$, $n = 4$), but no changes were found for mutant $\alpha 5$(S413F)^{HA} subunits (0.99 ± 0.08, $P = 0.963$, $n = 4$) (Fig. 3C, top). Furthermore, mutant $\alpha 5$(S413F)^{HA} subunits had a dominant negative effect by decreasing the trafficking of partnering $\beta 3$ (0.65 ± 0.06, $P = 0.0003$, $n = 4$) and $\gamma 2$ (0.65 ± 0.06, $P = 0.0106$, $n = 4$) subunits to the surface (Fig. 3C, middle and bottom). Mutant $\alpha 5$(S413F)^{HA} subunits had a dominant negative effect solely on $\beta 3$ subunits (0.83 ± 0.01, $P = 0.0423$, $n = 4$), with no significant changes in $\gamma 2$ subunits (0.86 ± 0.09, $P = 0.3928$, $n = 4$).

To determine to what extent mutant $\alpha 5$(V294F) and $\alpha 5$(S413F) subunits reduced biogenesis of GABA$_A$ receptors, whole-cell lysates were analysed by western blot (Fig. 3D). Total levels of mutant $\alpha 5$(V294F)^{HA} (0.59 ± 0.16, $P = 0.0611$, $n = 4$), and co-expressed $\beta 3$
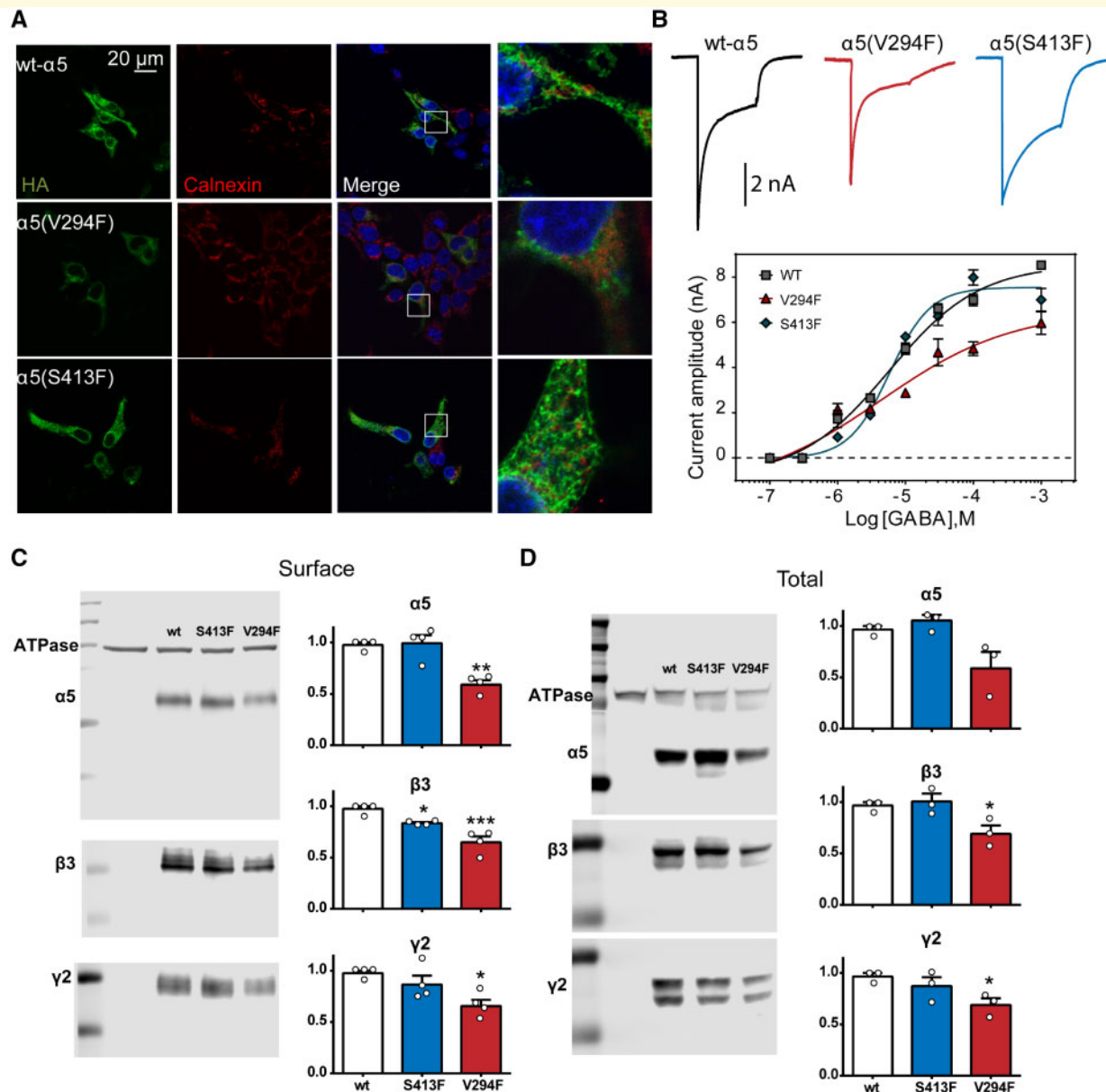
Figure 3 Mutant α5 subunits associated with *de novo* EOEE and co-expressed with β3 and γ2 subunits were trafficked to the cell surface as functional receptors in HEK293T cells. (**A**) Wild-type α5[HA] subunits or mutant α5(V294F)[HA] or α5(S413F)[HA] subunits were co-expressed with β3 and γ2 subunits in HEK293T cells. The transfected cells were permeabilized, and wild-type and mutant α5[HA] subunits were labelled with anti-HA antibodies (green). The ER was visualized with anti-calnexin antibody (red). White boxes on the merged images depict the enlarged area shown in the images to the *right*. Also shown are DAPI nuclear counterstaining (blue) and merge of the staining. (**B**) Representative GABA-evoked current traces obtained following rapid application of 1 mM GABA for 4 s to lifted HEK293T cells voltage clamped at −20 mV are shown at the *top* of the panel, and concentration-response curves obtained for wild-type α5 and mutant α5(V294F) and α5(S413F) subunit-containing α5β3γ2 GABAA receptors are shown at the *bottom* of the panel. (**C** and **D**) Surface (**C**) and total (**D**) levels of wild-type α5[HA] or mutant α5(V294F)[HA] and α5(S413F)[HA] subunits co-expressed with β3 and γ2 subunits in HEK293T cells. Band intensity of surface and total expressed α5, β3 and γ2 subunits were normalized to the ATPase signal, and the summarized data are shown in the bar graphs. Values are expressed as mean ± SEM (see text). One-way ANOVA with Dunnett's post-test was used to determine significance compared to the wild-type condition.

(0.69 ± 0.08, $P = 0.0489$, $n = 4$) and γ2 (0.69 ± 0.07, $P = 0.0429$, $n = 4$) subunits were all reduced; in contrast, expression of mutant α5(S413F)[HA]β3γ2 subunits did not differ from those of wild-type subunits (α5 1.05 ± 0.05,

$P = 0.7668$; β3 1.01 ± 0.08, $P = 0.8874$; γ2 0.87 ± 0.09, $P = 0.5320$, $n = 4$). Similar findings were found in hippocampal neurons transfected with α5(V294F) and α5(S413F) subunits (data not shown).

Two novel *GABRA1* mutations associated with EOEE caused overall reduction of GABAergic synapses of hippocampal neurons

Following the same approach as described above, we sought to determine the synaptic distribution of the mutant $\alpha1$(P260S) and $\alpha1$(L296S/W315L) subunits. Thus, we expressed HA fusion proteins encoding wild-type $\alpha1^{HA}$ or mutant $\alpha1$(P260S)^{HA} or $\alpha1$(L296S/W315L)^{HA} subunits in hippocampal neurons cultured for DIV 12 (Fig. 4A). We found major decreases in HA-stained dendritic puncta for both mutant $\alpha1$(P260S)^{HA} and $\alpha1$(L296S/W315L)^{HA} subunits transfected into hippocampal neurons compared with wild-type $\alpha1^{HA}$ subunit-containing neurons, which displayed a clear pattern of HA-stained synaptic contacts around the dendrites (Fig. 4A). As expected, reduction of dendritic expression of mutant $\alpha1$(P260S)^{HA} and $\alpha1$(L296S/W315L)^{HA} subunits significantly decreased the efficacy of GABAergic inhibition of hippocampal neurons (Fig. 4B). In comparison to wild-type $\alpha1$ subunit-containing neurons (40.6 ± 2.4 pA, $n = 5$), the amplitudes of mIPSCs in neurons expressing mutant $\alpha1$(P260S) (29.9 ± 1.9 pA, $P = 0.0069$, $n = 5$) or $\alpha1$(L296S/W315L) (29.3 ± 1.9 pA, $P = 0.0046$, $n = 5$) subunits were reduced (Fig. 4B, bottom left). In addition, transfection of either mutant $\alpha1$(P260S) or $\alpha1$(L296S/W315L) subunits resulted in faster mIPSC decay times (90.39 ± 4.37 ms, $P = 0.0425$, $n = 5$; 69.93 ± 2.44 ms, $P = 0.0002$, $n = 5$) and slower rise times (3.59 ± 1.10 ms, $P = 0.1793$, $n = 5$; 7.23 ± 1.15 ms, $P = 0.0014$, $n = 5$) relative to those recorded in hippocampal neurons transfected with wild-type $\alpha1$ subunits (decay time, 106.6 ± 5.8 ms; rise time, 1.23 ± 0.41 ms, $n = 5$) (Fig. 4B, bottom middle and right).

Next, we sought to determine whether the preferential distribution of mutant $\alpha1$(P260S) and $\alpha1$(L296S/W315L) subunits in the somata of hippocampal neurons (Fig. 4A) was due impaired biogenesis of GABA$_A$ receptors containing mutant $\alpha1$ subunits, which could result in the retention of mutant $\alpha1$ subunits in the ER (Fig. 4C). We found that both mutant $\alpha1$(P260S) (MCC = 0.73 ± 0.04, $n = 3$, $P = 0.0010$) and $\alpha1$(L296S/W315L) (MCC = 0.66 ± 0.02, $n = 3$, $P = 0.0045$) subunits were substantially co-localized with calnexin in the ER ($\alpha1$ wild-type MCC = 0.45 ± 0.03, $n = 3$). Although these results suggest that a fraction of the receptors was retained in the ER, functional data showed that a significant fraction of GABA$_A$ receptors containing mutant $\alpha1$ subunits were effectively trafficked to the membrane forming functional receptors (Fig. 4D). Macroscopic peak GABA-evoked currents recorded from HEK293T cells co-transfected with $\beta3$, $\gamma2$ and mutant $\alpha1$(P260S) or $\alpha1$(L296S/W315L) subunits were both decreased by $\sim60\%$ (3430 ± 255 pA, $n = 29$, $P = 0.0001$; 3913 ± 118 pA, $n = 19$, $P = 0.0001$), relative to wild-type currents (9071 ± 273 pA, $n = 31$). In addition, currents recorded from co-transfected cells with mutant $\alpha1$(P260S) subunits had unchanged GABA potency and had GABA concentration-response curves with EC$_{50}$'s similar to those of wild-type $\alpha1\beta3\gamma2$ GABA$_A$ receptors [EC$_{50}^{(P260S)}$ = $19.9\,\mu$M, $P = 0.8020$, $n = 29$; EC$_{50}^{(WT)}$ = $25.6\,\mu$M, $n = 31$]. Conversely, currents recorded from co-transfected cells with the mutant $\alpha1$(L296S/W315L) subunit had a ~5-fold increase in GABA$_A$ receptor potency (EC$_{50}$ = $5.03\,\mu$M, $P = 0.0001$, $n = 19$). To determine whether the differences found in GABA potency were due to an increase in the fraction of binary $\alpha\beta$ receptors of mutant $\alpha1$(L296S/W315L) GABA$_A$ receptors, the fractional Zn^{2+} inhibition was measured. Whereas receptors containing mutant $\alpha1$(P260S) subunits displayed a fractional Zn^{2+} inhibition that resembled that of wild-type $\alpha1\beta3\gamma2$ receptors ($7 \pm 1\%$, $n = 7$, $P = 0.8567$; $8 \pm 1\%$, $n = 16$, respectively), currents recorded from receptors containing mutant $\alpha1$(L296S/W315L) subunits had significantly increased Zn^{2+} sensitivity ($34 \pm 2\%$, $n = 7$, $P = 0.0001$).

Two novel EOEE mutant $\alpha1$ subunits decreased both surface and total levels of $\alpha1$ subunits

We co-expressed $\beta3$, $\gamma2$ and either wild-type $\alpha1$, mutant $\alpha1$(P260S) or mutant $\alpha1$(L296S/W315L) subunits in HEK293T cells and assessed surface and total expression levels of $\beta3$, $\gamma2$ and $\alpha1$ subunits (Fig. 4E and F). Co-transfection of mutant $\alpha1$(P260S) subunits with $\beta3$ and $\gamma2$ subunits decreased surface $\alpha1$ subunit levels (0.55 ± 0.04, $n = 4$, $P = 0.0001$) (Fig. 4E, top), with no effect on surface $\beta3$ subunit levels (0.94 ± 0.09, $n = 4$, $P = 0.9799$) (Fig. 4E, middle) or surface $\gamma2$ subunit levels (0.87 ± 0.04, $n = 4$, $P = 0.3162$) (Fig. 4E, bottom). Co-transfection of mutant $\alpha1$(L296S/W315L) subunits with $\beta3$ and $\gamma2$ subunits decreased surface $\alpha1$ subunit levels (0.36 ± 0.03, $n = 7$, $P = 0.0001$) (Fig. 4E, top) and decreased surface $\beta3$ subunit levels (0.81 ± 0.03, $n = 7$, $P = 0.0353$) (Fig. 4E, middle), with no effect on surface $\gamma2$ levels (0.85 ± 0.02, $n = 7$, $P = 0.0764$) (Fig. 4E, bottom).

Co-transfection of mutant $\alpha1$(P260S) subunits with $\beta3$ and $\gamma2$ subunits decreased total $\alpha1$ subunit levels (0.69 ± 0.04, $n = 5$, $P = 0.0028$) (Fig. 4F, top), with no effect on total $\beta3$ subunit levels (1.08 ± 0.04, $n = 5$, $P = 0.9491$) (Fig. 4F, middle) or total $\gamma2$ subunit levels (1.02 ± 0.04, $n = 5$, $P = 0.9979$) (Fig. 4F, bottom). Co-transfection of mutant $\alpha1$(L296S/W315L) subunits with $\beta3$ and $\gamma2$ subunits decreased total $\alpha1$ subunit levels (0.33 ± 0.06, $n = 5$, $P = 0.0001$) (Fig. 4F, top), with no effect on total $\beta3$ subunit levels (0.80 ± 0.14, $n = 5$, $P = 0.7042$) (Fig. 4F, middle) or total $\gamma2$ subunit levels (0.90 ± 0.15, $n = 5$, $P = 0.9822$) subunits (Fig. 4F, bottom). Similar findings were found in hippocampal neurons transfected with $\alpha1$(P260S) and $\alpha1$(L296S/W315L) subunits (data not shown).

Figure 4 Two novel EOEE mutant α1 subunits caused an overall reduction of GABAergic IPSCs in hippocampal neurons in cell culture. (**A**) Hippocampal neurons were transfected with wild-type (wt) α1[HA] subunits or mutant α1(P260S)[HA] or α1(L296S/W315L)[HA] subunits and fixed 48 h later. Neurons were stained with anti-HA (red) and anti-MAP2 (green) antibodies. Staining patterns were characterized using confocal microscopy. The *right* of the panel contains enlarged images of the neurites in white boxes. (**B**) Representative mISPCs recorded at −60 mV in cultured hippocampal neurons over-expressing wild-type α1[HA] subunits or mutant α1(P260S)[HA] or α1(L296S/W315L)[HA] subunits are presented. *Bottom* graphs represent summarized mISPC data. Values are expressed as mean ± SEM (see text). One-way ANOVA with Dunnett's post-test was used to determine significance compared to the wild-type condition. (**C**) Wild-type α1[HA] subunits or mutant α1(P260S)[HA] or

Three de novo GABRA1 mutations were relatively frequently found in cases with EOEE

Previously, five unrelated cases carrying the GABRA1 mutation c.G335A, p.R112Q (Carvill et al., 2014; Johannesen et al., 2016; Kodera et al., 2016), and one case carrying the GABRA1 mutation c.A343G, p.N115D (Johannesen et al., 2016) were found in EOEE, but functional studies have not been reported for either of these mutations. We report two additional cases carrying these mutations (Tables 1 and 3). An aspect that draws attention to these two mutations, and unlike the previous ones described above, these mutations were found in the N-terminal region of GABA$_A$ receptors, which means that they are likely in part of the GABA binding domain. We determined the functional consequences of the α1(R112Q) and α1(N115D) subunit amino acid substitutions by measuring macroscopic GABA-evoked currents from cells co-transfected with wild-type or mutant α1 subunits and β3 and γ2 subunits (Fig. 5A, top). Unexpectedly, no changes were found in peak GABA-evoked current amplitudes recorded from receptors containing mutant α1(R112Q) or α1(N115D) subunits (8167 $\pm$ 346 pA, n = 17, P = 0.2122; 7878 $\pm$ 625 pA, n = 19, P = 0.0668), relative to wild-type receptor currents (9071 $\pm$ 273 pA, n = 31). Since these mutations are located in the GABA binding domain, it is likely that these mutations disrupted coupling of GABA binding to channel gating leading to altered GABA potency. Accordingly, both mutant α1(R112Q) and α1(N115D) subunits caused a 2–5-fold decrease in GABA$_A$ receptor potency (EC$_{50}^{(R112Q)}$ = 48.3 μM, n = 10, P = 0.0235; EC$_{50}^{(N115D)}$ = 126 μM, n = 10, P = 0.0001) relative to that of wild-type receptors (EC$_{50}$ = 25.6 μM, n = 31) (Fig. 5A, bottom left). Moreover, consistent with the functional data, none of the mutations reduced surface or total levels of α1 subunits (surface: R112Q, 1.04 $\pm$ 0.09, n = 4, P = 0.9261; N115D, 1.03 $\pm$ 0.03, n = 7, P = 0.9419; total: R112Q, 0.99 $\pm$ 0.06, n = 5, P = 0.9997; N115D, 1.03 $\pm$ 0.07, n = 5, P = 0.9657), β3 subunits (surface: R112Q, 0.93 $\pm$ 0.09, n = 4, P = 0.9485; N115D, 1.03 $\pm$ 0.03, n = 7, P = 0.9512. total: R112Q, 1.04 $\pm$ 0.04, n = 5, P = 0.9961; N115D, 0.98 $\pm$ 0.13, n = 5, P = 0.9999) or γ2 subunits (surface: R112Q, 0.92 $\pm$ 0.05, n = 4, P = 0.7917; N115D, 0.96 $\pm$ 0.04, n = 7, P = 0.9936;

total: R112Q, 1.08 $\pm$ 0.05, n = 5, P = 0.9081; N115D, 1.05 $\pm$ 0.07, n = 5, P = 0.9840) subunits (Fig. 5C and D).

Further, two unrelated cases with Ohtahara and West syndromes were found with the de novo GABRA1 p.P260L mutation (Kodera et al., 2016), which is at the same position of the mutant α1(P260S) subunit described above. Similar to the mutant α1(P260S) subunit (Fig. 4D), co-transfection of mutant α1(P260L) subunits with β3 and γ2 subunits decreased macroscopic GABA-evoked currents by $\sim$60% (2762 $\pm$ 174 pA, n = 14, P = 0.0001) (Fig. 5A), did not alter GABA potency (38.3 μM, P = 0.5444, n = 6), and did not alter fractional Zn^{2+} inhibition (7 $\pm$ 1%, n = 6, P = 0.9999). Conversely, the mutant α1(P260L) subunit did not affect surface or total expression of α1 subunits (surface: 0.85 $\pm$ 0.08, n = 4, P = 0.1868; total: 0.80 $\pm$ 0.04, n = 5, P = 0.1007), β3 subunits (surface: 0.91 $\pm$ 0.06, n = 4, P = 0.7861; total: 1.04 $\pm$ 0.04, n = 5, P = 0.9949) or γ2 subunits (surface: 0.94 $\pm$ 0.04, n = 4, P = 0.9458; total: 1.06 $\pm$ 0.07, n = 5, P = 0.9503) subunits (Fig. 5C and D, left).

In addition, we studied the mutations that are part of the compound mutant α1(L296S/W315L) subunit to gain insight into whether there were differences in the functional and/or expression properties of receptors with α1 subunits containing these single point mutations. Resembling the compound mutant, receptors containing either mutant α1(L296S) or α1(W315L) subunit reduced GABA-evoked currents to $\sim$70 to 50% (4702 $\pm$ 396 pA, n = 14, P = 0.0001; 6150 $\pm$ 311 pA, n = 14, P = 0.0001) relative to control currents (9071 $\pm$ 273 pA, n = 31) (Fig. 5A, top). However, mutant α1(L296S) subunits did not change GABA$_A$ receptor potency (10.9 μM, P = 0.0764, n = 10), while mutant α1(W315L) subunits had GABA concentration-response curves with EC$_{50}$'s similar to those found with the compound α1(L296S/W315L)β3γ2 subunits (7.02 μM, P = 0.0001, n = 8) (Fig. 5A, bottom right).

Comparison of fractional Zn^{2+} inhibition demonstrated that receptors containing mutant α1(L296S) or α1(W315L) subunits had an increased Zn^{2+} sensitivity (16 $\pm$ 3%, n = 9, P = 0.0018; 13 $\pm$ 1%, n = 8, P = 0.0748) relative to control receptors (8 $\pm$ 1%, n = 16), which suggested trafficking deficiency of α1β3γ2 receptors containing mutant subunits to the cell surface and increase in

Figure 4 Continued
α1(L296S/W315L)^{HA} subunits were co-expressed with β3 and γ2 subunits in HEK293T cells. The transfected cells were permeabilized, and wild-type and mutant α1^{HA} subunits were labelled with anti-HA antibodies (green). The ER was visualized with anti-calnexin antibody (red). White boxes on the merged images depicted the enlarged area shown in the images to the right. Also shown was DAPI nuclear counterstaining (blue) and the merge of the stainings. (**D**) Representative GABA-evoked current traces obtained following rapid application of 1 mM GABA for 4 s to lifted HEK293T cells voltage clamped at -20 mV are shown at the top of the panel. Concentration-response curves were obtained for wild-type α1 or mutant α1(P260S) or α1(L296S/W315L) subunit-containing α1β3γ2 GABA$_A$ receptors. (**E and F**) Surface (**E**) and total (**F**) levels of wild-type α1 or mutant α1(P260S) or α1(L296S/W315L) subunits co-expressed with β3 and γ2 subunits in HEK293T cells are presented. Band intensity of surface and total expressed α1, β3 and γ2 subunits were normalized to the ATPase signal, and the summarized data are shown in the bar graphs. Values are expressed as mean $\pm$ SEM (see text). One-way ANOVA with Dunnett's post-test was used to determine significance compared to the wild-type condition.
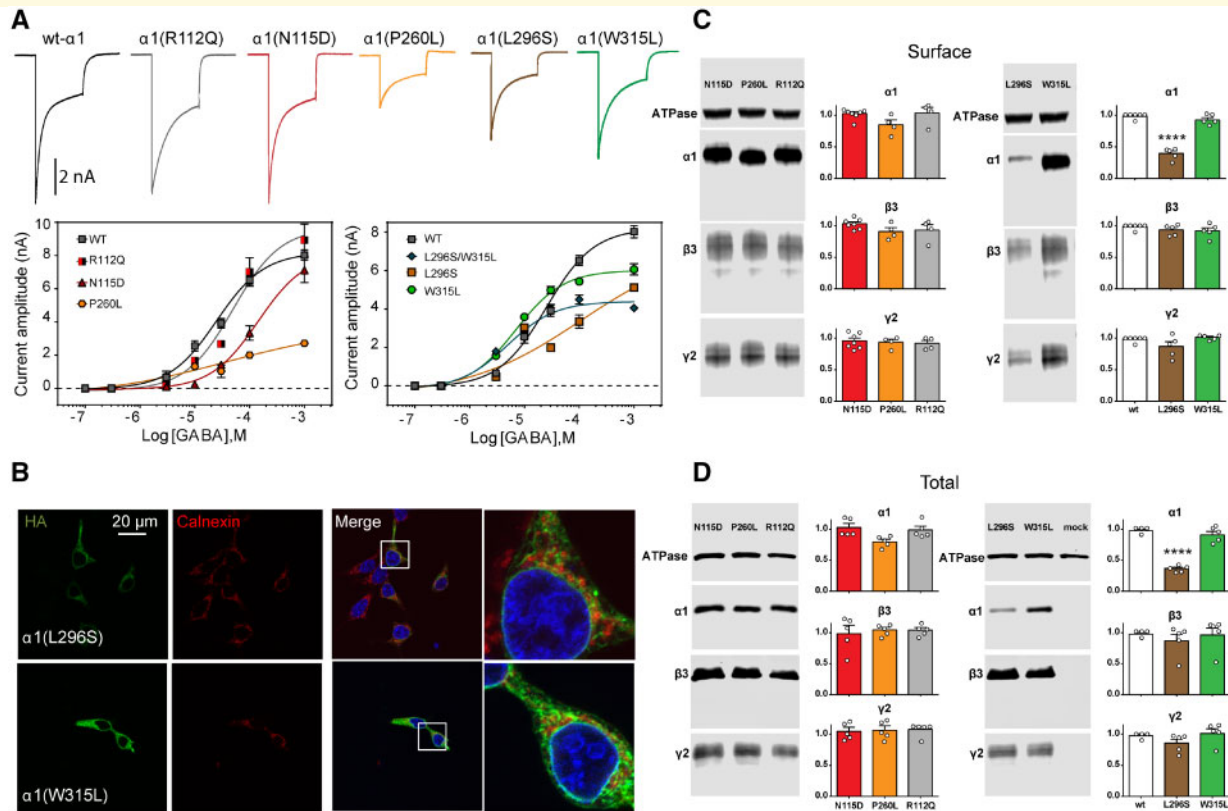
Figure 5 Three *de novo* mutations in *GABRA1* found in several cases with EOEE cause divergent effects in GABA$_A$ receptor function. (**A**) Representative GABA-evoked current traces obtained following rapid application of 1 mM GABA for 4 s to lifted HEK293T cells voltage clamped at −20 mV are shown at the *top* of the panel. Concentration-response curves were obtained for wild-type (wt) α1 or mutant α1(R112Q), α1(N115D), α1(P260L), α1(L296S) or α1(W315L) subunit-containing α1β3γ2 GABA$_A$ receptors are shown at the *bottom* of the panel. (**B**) Wild-type α1^{HA} subunits or mutant α1^{HA}(L296S) or α1^{HA}(W315L) subunits were co-expressed with β3 and γ2 subunits in HEK293T cells. α1^{HA} subunits were labelled with anti-HA antibody (green), and the ER was visualized with anti-calnexin antibody (red). White boxes on the merged images depict the enlarged area shown in the images to the *right*. Also shown are DAPI nuclear counterstaining (blue) and merge of the staining. (**C** and **D**) Surface (**C**) and total (**D**) levels of wild-type and mutant α1(R112Q), α1(N115D), α1(P260L), α1(L296S) and α1(W315L) subunits co-expressed with β3 and γ2 subunits in HEK293T cells are shown. Band intensity of surface and total expressed α1, β3 and γ2 subunits were normalized to the ATPase signal, and the summarized data are shown in the bar graphs. Values are expressed as mean ± SEM (see text). One-way ANOVA with Dunnett's post-test was used to determine significance compared to the wild-type condition.

trafficking of α1β3 Zn^{2+} sensitive receptors to the cell surface. Therefore, HEK293T cells were permeabilized and immunolabelled with anti-HA and anti-calnexin antibodies to assess retention of mutant α1(L296S) and α1(W315L) receptors in the ER. Similar to the ER retention shown by mutant α1(L296S/W315L) subunits (Fig. 4C), mutant α1^{HA}(L296S) subunits co-localized with calnexin. In contrast, mutant α1^{HA}(W315L) subunits spread outside the ER (Fig. 5B). In addition, only mutant α1(L296S) receptors decreased surface (L296S, 0.40 ± 0.04, $n = 5$, $P = 0.0001$; W315L, 0.93 ± 0.03, $n = 5$, $P = 0.8637$) and total (L296S, 0.37 ± 0.02, $n = 5$, $P = 0.0001$; W315L, 0.91 ± 0.05, $n = 5$, $P = 0.9143$) α1 subunit levels (Fig. 5C and D, right). Neither of the mutant α1(L296S) and α1(W315L) receptors reduced surface (L296S, 0.93 ± 0.04, $n = 5$, $P = 0.9485$; W315L, 0.92 ± 0.05, $n = 5$, $P = 0.8580$) or total (L296S, 0.87 ± 0.10, $n = 5$, $P = 0.9518$; W315L, 0.96 ± 0.11,

$n = 5$, $P = 0.9999$) β3 subunit levels or surface (L296S, 0.87 ± 0.07, $n = 5$, $P = 0.2217$; W315L, 1.01 ± 0.02, $n = 5$, $P = 0.9940$) or total (L296S, 0.86 ± 0.07, $n = 5$, $P = 0.8309$; W315L, 1.01 ± 0.08, $n = 5$, $P = 0.9995$) γ2 subunit levels.

Discussion

Several studies have described the association of EOEE with *de novo* mutations in neurotransmitter receptors, synaptic proteins, and voltage- and ligand-gated ion channels; however, little is known about the molecular mechanisms that lead to the disease. Interestingly, despite the multiplicity of targets that have been associated with the disease, ultimately all of them lead to an imbalance in neuronal excitability. Undoubtedly, differences in expression level

and signalling pathways, and specificity in brain regions create the broad spectrum of symptoms that characterize the phenotypic diversity of EOEE. Mutations in GABRs are frequently associated with genetic epilepsy syndromes (Kang and Macdonald, 2016). More than 60 reported sporadic *de novo* mutations in *GABRA1*, *GABRB1–3*, and *GABRG2* have been found to be linked to the severe EOEEs (Ohtahara syndrome, infantile spasms, Doose syndrome and Dravet syndrome). To a certain extent, different mutations in the same GABR produce different epilepsy syndromes commonly associated with haploinsufficiency and hyperexcitability (Allen *et al.*, 2013; Carvill *et al.*, 2014; Srivastava *et al.*, 2014; Papandreou *et al.*, 2015; Reinthaler *et al.*, 2015; Zhang *et al.*, 2015; Johannesen *et al.*, 2016; Kodera *et al.*, 2016; Lien *et al.*, 2016; Baldridge *et al.*, 2017; Hamdan *et al.*, 2017; Hernandez *et al.*, 2017*a*, *b*; Ishii *et al.*, 2017; Moller *et al.*, 2017; Shen *et al.*, 2017; Heyne *et al.*, 2018).

Most of the GABA$_A$ receptor α1, β(1,2,3) and γ2 subunit residue substitutions associated with severe epilepsy phenotypes occur more frequently in the pore-forming domain of the receptor critical for GABA$_A$ receptor activation (Bianchi *et al.*, 2001; Bianchi and Macdonald, 2002; Althoff *et al.*, 2014; Laverty *et al.*, 2019; Masiulis *et al.*, 2019), where they are more likely to cause impaired receptor function (Janve *et al.*, 2016; Hernandez *et al.*, 2017*a*, *b*; Ishii *et al.*, 2017; Shen *et al.*, 2017).

We have demonstrated common impairments caused by *de novo* GABR mutations including impaired receptor biogenesis (impaired gene transcription, subunit translation, subunit folding, receptor assembly, receptor cell surface trafficking and surface stability), impaired agonist binding and impaired channel gating (Janve *et al.*, 2016; Hernandez *et al.*, 2017*a*, *b*; Ishii *et al.*, 2017; Shen *et al.*, 2017). In the present study, we demonstrated that mutations in *GABRA5* and *GABRA1* found in cases with EOEE were accompanied by a reduced amplitude of GABA$_A$ receptor mediated mIPSCs and altered synaptic clustering and distribution in hippocampal neurons. Our data suggested a decrease in the number of active postsynaptic receptors that could weaken synaptic efficacy. As GABA$_A$ receptor clustering at inhibitory synapses is likely to modulate network excitability during brain development (Petrini *et al.*, 2014), our results suggested that a 'hyperexcitability syndrome' can be caused additionally by altered distribution of mutant receptors at postsynaptic sites.

Synaptic strength is tuned by efficient clustering and distribution of GABA$_A$ receptors composed of different subunits at inhibitory synapses, which in turn are highly regulated by postsynaptic scaffolding proteins (Essrich *et al.*, 1998; Jacob *et al.*, 2005; Tretter *et al.*, 2008; Luscher *et al.*, 2011; Choii and Ko, 2015). Gephyrin was described as the major candidate protein for synaptic α1, α2, α3, β2/3 and γ2 GABA$_A$ receptor subunit clustering, although α5 subunits were found to be recruited by gephyrin (Christie and de Blas, 2002; Serwanski *et al.*, 2006). Further, previous studies found that gephyrin

knockout mice had loss of synaptic GABA$_A$ receptor clusters containing α2, α3, β2/3 and γ2, subunits, but α1 and α5 subunits were unaltered (Kneussel *et al.*, 1999), while GABA$_A$ receptor γ2 subunit knockout mice had reduced gephyrin-dependent clustering of postsynaptic GABA$_A$ receptors (Essrich *et al.*, 1998). Thus, it is expected that α1, α2, α3, β2/3 and γ2 GABA$_A$ receptor subunits solely contribute to the postsynaptic gephyrin-dependent clustering. Conversely, clustering of α5 subunits depends on the location of these receptors, either at synaptic or extrasynaptic sites (Brunig *et al.*, 2002; Christie and de Blas, 2002; Serwanski *et al.*, 2006). Accordingly, GABA$_A$ receptors containing α5 subunits at synapses are clustered by gephyrin (Christie and de Blas, 2002; Serwanski *et al.*, 2006) and at extrasynaptic sites by radixin (Loebrich *et al.*, 2006). We found that EOEE-associated mutant α5(V294F) and α5(S413F) subunits significantly increased synaptic recruitment of the scaffold protein gephyrin at synapses in hippocampal neurons. In contrast, EOEE-associated mutant α1(P260S) and α1(L296S/ W315L) subunits were lost from synaptic sites and were localized almost exclusively in the soma. Our data suggested that clustering of GABA$_A$ receptors containing mutant α1 and α5 subunits at synapses represented two active functional pools of receptors that were mobilized and clustered at GABAergic synapses in a gephyrin-dependent manner and were likely to modulate network excitability in EOEE.

For the most part, all patients carrying pathogenic *de novo* mutations in *GABRA1* have been reported to have a wide phenotypic range of severe epileptic encephalopathies (Johannesen *et al.*, 2016; Kodera *et al.*, 2016). Remarkably, we found that there is a recurrence of the same mutations in different subunits in the structural domains of the receptor linked to the specific functions, which are commonly found between the N-terminal extracellular domain and the pore that are critical for GABA$_A$ receptor activation (Bianchi *et al.*, 2001; Bianchi and Macdonald, 2002; Laverty *et al.*, 2019; Masiulis *et al.*, 2019). Thus, the α1 subunit substitutions P260S and P260L occurred at a homologous position in the γ2 subunit (P282S) found in patients with epileptic encephalopathies (Shen *et al.*, 2017). In addition, the α1 subunit substitution (N115D) also occurred at the homologous position in β3 subunits (N110D) found in a patient with infantile spasms (Allen *et al.*, 2013; Janve *et al.*, 2016). In the same way, the α5 subunit substitution (V294F) also occurred at the homologous position of the α1 subunit (V287L) found in a patient with EOEE (Kodera *et al.*, 2016), and a recurrent variant in the same position of V294 but replaced by a leucine (V294L) was found in a case with delayed motor and cognitive development (Butler *et al.*, 2018). Therefore, identification of patients carrying *de novo* pathogenic mutations in *GABRA5* is remarkable. We previously described GABA$_A$ receptor gating defects in three rare mutations in *GABRA5* (c.610G>A, p.V204I, c.838T>C, pW280R, c.1358C>T, p.P453L) found in individuals with sporadic genetic epilepsy (Klassen *et al.*, 2011; Hernandez *et al.*,

2016). Later, similar findings were reported in an exome-based case-control study of rare variants in *GABRA5* in cases clinically evaluated for genetic generalized epilepsy (May *et al.*, 2018). Another study reported two rare missense mutations in *GABRA5* (c.610G>A, p.V204I, c.338G>C, pG113A) in autism spectrum disorder cases (Zurek *et al.*, 2016).

This was a deep functional study of *GABRA5* and *GABRA1 de novo* mutations by use of primary hippocampal neurons and non-neuronal cells. We found that *GABRA5* and *GABRA1* mutations impaired GABA$_A$ receptor function and biogenesis, and GABA$_A$ receptor immobilization and accumulation by gephyrin at the synapse. Overall these findings demonstrate the recurrence of multiple mutations and variants in common structural 'hot spots' in the receptor that are likely to cause impairment of GABAergic function. Our studies reveal new molecular mechanisms that might lead to the neurological dysfunction found in patients who carry mutations in *GABRA5* and *GABRA1*, complementing the prevailing GABAergic channelopathy paradigm in EOEE.

Acknowledgements

Funding

Competing interests

The authors declare no competing financial interests.

Supplementary material

Supplementary material is available at *Brain* online.

References

Abecasis GR, Auton A, Brooks LD, DePristo MA, Durbin RM, Handsaker RE, et al. An integrated map of genetic variation from 1,092 human genomes. Nature 2012; 491: 56–65.

Adzhubei IA, Schmidt S, Peshkin L, Ramensky VE, Gerasimova A, Bork P, et al. A method and server for predicting damaging missense mutations. Nat Methods 2010; 7: 248–9.

Aken BL, Ayling S, Barrell D, Clarke L, Curwen V, Fairley S, et al. The Ensembl gene annotation system. Database 2016; 2016: baw093.

Allen AS, Berkovic SF, Cossette P, Delanty N, Dlugos D, Eichler EE, et al. *De novo* mutations in epileptic encephalopathies. Nature 2013; 501: 217–21.

Althoff T, Hibbs RE, Banerjee S, Gouaux E. X-ray structures of GluCl in apo states reveal a gating mechanism of Cys-loop receptors. Nature 2014; 512: 333–7.

Axeen EJT, Olson HE. Neonatal epilepsy genetics. Sem Fetal Neonatal Med 2018; 23: 197–203.

Baldridge D, Heeley J, Vineyard M, Manwaring L, Toler TL, Fassi E, et al. The Exome Clinic and the role of medical genetics expertise in the interpretation of exome sequencing results. Genet Med 2017; 19: 1040–8.

Bianchi MT, Haas KF, Macdonald RL. Structural determinants of fast desensitization and desensitization-deactivation coupling in GABA$_A$ receptors. J Neurosci 2001; 21: 1127–36.

Bianchi MT, Macdonald RL. Slow phases of GABA(A) receptor desensitization: structural determinants and possible relevance for synaptic function. J Physiol 2002; 544(Pt 1): 3–18.

Brunig I, Scotti E, Sidler C, Fritschy JM. Intact sorting, targeting, and clustering of gamma-aminobutyric acid A receptor subtypes in hippocampal neurons in vitro. J Comparat Neurol 2002; 443: 43–55.

Butler KM, Moody OA, Schuler E, Coryell J, Alexander JJ, Jenkins A, et al. *De novo* variants in *GABRA2* and *GABRA5* alter receptor function and contribute to early-onset epilepsy. Brain 2018; 141: 2392–405.

Carvill GL, Weckhuysen S, McMahon JM, Hartmann C, Moller RS, Hjalgrim H, et al. *GABRA1* and *STXBP1*: novel genetic causes of Dravet syndrome. Neurology 2014; 82: 1245–53.

Choii G, Ko J. Gephyrin: a central GABAergic synapse organizer. Exp Mol Med 2015; 47: e158.

Christie SB, de Blas AL. alpha5 Subunit-containing GABA(A) receptors form clusters at GABAergic synapses in hippocampal cultures. Neuroreport 2002; 13: 2355–8.

Connolly CN, Krishek BJ, McDonald BJ, Smart TG, Moss SJ. Assembly and cell surface expression of heteromeric and homomeric gamma-aminobutyric acid type A receptors. J Biol Chem 1996; 271: 89–96.

Du J, Lu W, Wu S, Cheng Y, Gouaux E. Glycine receptor mechanism elucidated by electron cryo-microscopy. Nature 2015; 526: 224–9.

Essrich C, Lorez M, Benson JA, Fritschy JM, Luscher B. Postsynaptic clustering of major GABA$_A$ receptor subtypes requires the gamma 2 subunit and gephyrin. Nat Neurosci 1998; 1: 563–71.

Hamdan FF, Myers CT, Cossette P, Lemay P, Spiegelman D, Laporte AD, et al. High rate of recurrent De Novo mutations in developmental and epileptic encephalopathies. Am J Hum Genet 2017; 101: 664–85.

Hamdan FF, Srour M, Capo-Chichi JM, Daoud H, Nassif C, Patry L, et al. *De novo* mutations in moderate or severe intellectual disability. PLoS Genet 2014; 10: e1004772.

Helbig I, Tayoun AA. Understanding genotypes and phenotypes in epileptic encephalopathies. Mol Syndromol 2016; 7: 172–81.

Helbig I, von Deimling M, Marsh ED. Epileptic encephalopathies as neurodegenerative disorders. Adv Neurobiol 2017; 15: 295–315.

Helbig KL, Farwell Hagman KD, Shinde DN, Mroske C, Powis Z, Li S, et al. Diagnostic exome sequencing provides a molecular diagnosis for a significant proportion of patients with epilepsy. Genet Med 2016; 18: 898–905.

Hernandez CC, Klassen TL, Jackson LG, Gurba K, Hu N, Noebels JL, et al. Deleterious rare variants reveal risk for loss of GABA$_A$ receptor function in patients with genetic epilepsy and in the general population. PLoS One 2016; 11: e0162883.

Hernandez CC, Kong W, Hu N, Zhang Y, Shen W, Jackson L, et al. Altered channel conductance states and gating of GABA$_A$ receptors by a pore mutation linked to Dravet syndrome. eNeuro 2017a; 4(1).

Hernandez CC, Zhang Y, Hu N, Shen D, Shen W, Liu X, et al. GABA A Receptor coupling junction and pore *GABRB3* mutations are linked to early-onset epileptic encephalopathy. Sci Rep 2017b; 7: 15903.

Heyne HO, Singh T, Stamberger H, Abou Jamra R, Caglayan H, Craiu D, et al. *De novo* variants in neurodevelopmental disorders with epilepsy. Nat Genet 2018; 50: 1048–53.

Hibbs RE, Gouaux E. Principles of activation and permeation in an anion-selective Cys-loop receptor. Nature 2011; 474: 54–60.

Huang X, Hernandez CC, Hu N, Macdonald RL. Three epilepsy-associated *GABRG2* missense mutations at the gamma+/beta- interface disrupt GABA$_A$ receptor assembly and trafficking by similar mechanisms but to different extents. Neurobiol Dis 2014; 68: 167–79.

Ishii A, Kang JQ, Schornak CC, Hernandez CC, Shen W, Watkins JC, et al. A *de novo* missense mutation of *GABRB2* causes early myoclonic encephalopathy. J Med Genet 2017; 54: 202–11.

Jacob TC, Bogdanov YD, Magnus C, Saliba RS, Kittler JT, Haydon PG, et al. Gephyrin regulates the cell surface dynamics of synaptic GABA$_A$ receptors. J Neurosci 2005; 25: 10469–78.

Janve VS, Hernandez CC, Verdier KM, Hu N, Macdonald RL. Epileptic encephalopathy de novo *GABRB* mutations impair GABA$_A$ receptor function. Ann Neurol 2016; 79: 806–25.

Johannesen K, Marini C, Pfeffer S, Moller RS, Dorn T, Niturad C, et al. Phenotypic spectrum of *GABRA1*: from generalized epilepsies to severe epileptic encephalopathies. Neurology 2016; 87: 1140–51.

Kang JQ, Macdonald RL. Molecular pathogenic basis for *GABRG2* mutations associated with a spectrum of epilepsy syndromes, from generalized absence epilepsy to Dravet syndrome. JAMA Neurol 2016; 73: 1009–16.

Klassen T, Davis C, Goldman A, Burgess D, Chen T, Wheeler D, et al. Exome sequencing of ion channel genes reveals complex profiles confounding personal risk assessment in epilepsy. Cell 2011; 145: 1036–48.

Kneussel M, Brandstatter JH, Laube B, Stahl S, Muller U, Betz H. Loss of postsynaptic GABA(A) receptor clustering in gephyrin-deficient mice. J Neurosci 1999; 19: 9289–97.

Kodera H, Ohba C, Kato M, Maeda T, Araki K, Tajima D, et al. *De novo GABRA1* mutations in Ohtahara and West syndromes. Epilepsia 2016; 57: 566–73.

Laverty D, Desai R, Uchanski T, Masiulis S, Stec WJ, Malinauskas T, et al. Cryo-EM structure of the human $\alpha1\beta3\gamma2$ GABA$_A$ receptor in a lipid bilayer. Nature 2019; 565: 516–20.

Le SV, Le PHT, Le TKV, Kieu Huynh TT, Hang Do TT. A mutation in *GABRB3* associated with Dravet syndrome. American journal of medical genetics Part A 2017; 173(8): 2126–31.

Lek M, Karczewski KJ, Minikel EV, Samocha KE, Banks E, Fennell T, et al. Analysis of protein-coding genetic variation in 60,706 humans. Nature 2016; 536: 285–91.

Lien E, Vatevik AK, Ostern R, Haukanes BI, Houge G. A second patient with a *De Novo GABRB1* mutation and epileptic encephalopathy. Ann Neurol 2016; 80: 311–2.

Loebrich S, Bahring R, Katsuno T, Tsukita S, Kneussel M. Activated radixin is essential for GABA$_A$ receptor alpha5 subunit anchoring at the actin cytoskeleton. EMBO J 2006; 25: 987–99.

Luscher B, Fuchs T, Kilpatrick CL. GABA$_A$ receptor trafficking-mediated plasticity of inhibitory synapses. Neuron 2011; 70: 385–409.

Masiulis S, Desai R, Uchanski T, Serna Martin I, Laverty D, Karia D, et al. GABA$_A$ receptor signalling mechanisms revealed by structural pharmacology. Nature 2019; 565: 454–9.

May P, Girard S, Harrer M, Bobbili DR, Schubert J, Wolking S, et al. Rare coding variants in genes encoding GABA$_A$ receptors in genetic generalised epilepsies: an exome-based case-control study. Lancet Neurol 2018; 17: 699–708.

McTague A, Howell KB, Cross JH, Kurian MA, Scheffer IE. The genetic landscape of the epileptic encephalopathies of infancy and childhood. Lancet Neurol 2016; 15: 304–16.

Miller PS, Aricescu AR. Crystal structure of a human GABA$_A$ receptor. Nature 2014; 512: 270–5.

Moller RS, Wuttke TV, Helbig I, Marini C, Johannesen KM, Brilstra EH, et al. Mutations in *GABRB3*: From febrile seizures to epileptic encephalopathies. Neurology 2017; 88: 483–92.

Ng PC, Henikoff S. Predicting deleterious amino acid substitutions. Genome Res 2001; 11: 863–74.

Nieh SE, Sherr EH. Epileptic encephalopathies: new genes and new pathways. Neurotherapeutics 2014; 11(4): 796–806.

Papandreou A, McTague A, Trump N, Ambegaonkar G, Ngoh A, Meyer E, et al. *GABRB3* mutations: a new and emerging cause of early infantile epileptic encephalopathy. Dev Med Child Neurol 2015; 58: 416–20.

Petrini EM, Ravasenga T, Hausrat TJ, Iurilli G, Olcese U, Racine V, et al. Synaptic recruitment of gephyrin regulates surface GABA$_A$ receptor dynamics for the expression of inhibitory LTP. Nat Commun 2014; 5: 3921.

Reinthaler EM, Dejanovic B, Lal D, Semtner M, Merkler Y, Reinhold A, et al. Rare variants in gamma-aminobutyric acid type A receptor genes in rolandic epilepsy and related syndromes. Ann Neurol 2015; 77: 972–86.

Schindelin J, Arganda-Carreras I, Frise E, Kaynig V, Longair M, Pietzsch T, et al. Fiji: an open-source platform for biological-image analysis. Nat Methods 2012; 9: 676–82.

Schwarz JM, Rodelsperger C, Schuelke M, Seelow D. MutationTaster evaluates disease-causing potential of sequence alterations. Nat Methods 2010; 7: 575–6.

Serwanski DR, Miralles CP, Christie SB, Mehta AK, Li X, De Blas AL. Synaptic and nonsynaptic localization of GABA$_A$ receptors containing the alpha5 subunit in the rat brain. J Comparat Neurol 2006; 499: 458–70.

Shen D, Hernandez CC, Shen W, Hu N, Poduri A, Shiedley B, et al. *De novo GABRG2* mutations associated with epileptic encephalopathies. Brain 2017; 140: 49–67.

Srivastava S, Cohen J, Pevsner J, Aradhya S, McKnight D, Butler E, et al. A novel variant in *GABRB2* associated with intellectual disability and epilepsy. Am J Med Genet Part A 2014; 164a: 2914–21.

Tretter V, Jacob TC, Mukherjee J, Fritschy JM, Pangalos MN, Moss SJ. The clustering of GABA(A) receptor subtypes at inhibitory synapses is facilitated via the direct binding of receptor alpha 2 subunits to gephyrin. J Neurosci 2008; 28: 1356–65.

Zhang Y, Kong W, Gao Y, Liu X, Gao K, Xie H, et al. Gene mutation analysis in 253 Chinese children with unexplained epilepsy and intellectual/developmental disabilities. PLoS One 2015; 10: e0141782.

Zurek AA, Kemp SW, Aga Z, Walker S, Milenkovic M, Ramsey AJ, et al. alpha5GABA$_A$ receptor deficiency causes autism-like behaviors. Ann Clin Transl Neurol 2016; 3: 392–8.